Hine, A.C., Feary, D.A., and Malone, M.J. (Eds.)
Proceedings of the Ocean Drilling Program, Scientific Results Volume 182

15. Data Report: Late Pleistocene Oxygen and Carbon Isotope Stratigraphy in Bulk- and Fine-Fraction Carbonate from the Great Australian Bight, ODP Leg 182, Site 1127[1]

Miriam S. Andres[2] and Judith A. McKenzie[2]

ABSTRACT

The aim of this study was to evaluate the potential of constructing an oxygen and carbon isotope stratigraphy for the late Pleistocene succession from Hole 1127B drilled on the Great Australian Bight. Stable isotope analyses were performed on bulk- and fine-fraction (<38 µm) sediment samples. The oxygen isotope variations are generally smaller in magnitude than expected from global pelagic records. This is most likely due to the neriticly dominated sediment composition. Correlation of the oxygen isotope data with carbonate mineralogy and downhole logging data shows simultaneous variations and trends, which are particularly evident in the mid-Pleistocene sediments. Correlation of the oxygen isotope data with the classic SPECMAP curve is used to evaluate the stratigraphic potential of the Site 1127 sediments. This study indicates that an isotope stratigraphy based on planktonic and benthic foraminifers is needed to fully evaluate the response of cool-water carbonates deposited in a margin setting to global ice–volume fluctuations and, hence, the associated sea level variations.

INTRODUCTION

Ocean Drilling Program (ODP) Leg 182 Site 1127 is the most seaward site of a three-site transect drilled through a set of prograding clino-

[1]Andres, M.S., and McKenzie, J.A., 2002. Data report: Late Pleistocene oxygen and carbon isotope stratigraphy in bulk- and fine-fraction carbonate from the Great Australian Bight, ODP Leg 182, Site 1127. *In* Hine, A.C., Feary, D.A., and Malone, M.J. (Eds.), *Proc. ODP, Sci. Results,* 182, 1–13 [Online]. Available from World Wide Web: <http://www-odp.tamu.edu/publications/182_SR/VOLUME/CHAPTERS/015.PDF>. [Cited YYYY-MM-DD]
[2]Geological Institute, ETH Zurich, CH-8092 Zurich, Switzerland.
Correspondence author: **miriam@erdw.ethz.ch**

Initial receipt: 29 November 2001
Acceptance: 10 May 2002
Web publication: 5 August 2002
Ms 182SR-015

forms immediately seaward of the present-day shelf edge on the Great Australian Bight (GAB) (Feary, Hine, Malone, et al., 2000). The site is located in 480.6 m of water, and drilling recovered 510.7 m of sediment with an average of 95% recovery. The upper 467 m of this neritic sediment wedge represents an extraordinarily thick Pleistocene succession that unconformably overlies the Pliocene–upper Miocene sediments at a distinct sequence boundary. The entire sedimentary succession is characterized by fine-grained bioturbated bioclastic carbonate wackestone to packstone. Based on shipboard magnetic data, the Bruhnes/Matuyama (B/M) boundary was placed at 343.4 meters below seafloor (mbsf).

Herein, we evaluate the potential to develop an oxygen isotope stratigraphy for Site 1127 based on $\delta^{18}O$ data compiled from bulk- and fine-fraction analyses. The fine fraction (defined as the <38-µm fraction) was identified by scanning electron microscope analysis as composed of calcareous nannoplankton and bioclastic sediment. We undertook the analysis of bulk sediment because it is far less labor intensive and, therefore, a less time-consuming method (Shackleton et al., 1993), which provides a rapid initial data set for evaluating the potential of conducting paleoceanographic research in cool-water open-marine carbonates.

METHODS AND PROCEDURES

Sample Preparation and Isotope Analysis

Splits of sediment samples from Hole 1127B were oven dried at 30°C and weighed. Approximately 1 cm^3 of material was ground for bulk stable isotope analyses. For fine-fraction analyses, a small split of the sample was sieved over a 38-µm stainless steel mesh sieve, and the fine fraction (<38 µm) was collected beneath. The collected sediment was then sonicated, filtered over a 0.45-µm membrane filter, and oven dried. Before isotopic analysis, ~0.5 mg of each sample was homogenized using a mortar and pestle. Stable isotope analysis of bulk- and fine-fraction samples was carried out at the Geological Institute (ETH Zurich) using a PRISM dual-inlet mass spectrometer. Results are expressed in the standard δ notation as per mil (‰) relative to the Peedee Belemnite cool-water carbonate standard. Instrument accuracy, referenced to an internal carbonate standard (Carrara marble), is 0.08‰ ± 0.03‰ (1 σ) for $\delta^{18}O$ and 0.05‰ ± 0.03‰ (1 σ) for $\delta^{13}C$. On average, 10 standards were measured during each run of 20 samples to determine precision for replicate analyses. The data are given in Table **T1** and graphically displayed in Figures **F1** and **F2.**

Mineralogical and Downhole Logging Data

All mineralogical X-ray diffraction data and downhole logging data presented in Figure **F3** were acquired on board the *JOIDES Resolution* (Feary, Hine, Malone, et al., 2000). Analytical procedures are discussed in the Leg 182 *Initial Reports* volume (Feary, Hine, Malone, et al., 2000). For the downhole natural gamma ray (NGR) measurement, the data were smoothed using a five-point running average. The upper 80 m was logged through the pipe, and values were multiplied by a factor of 5 for comparable amplitudes.

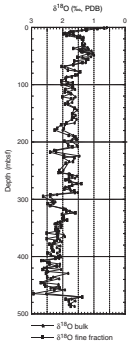

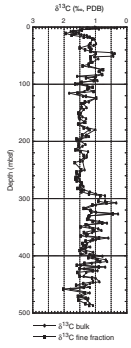

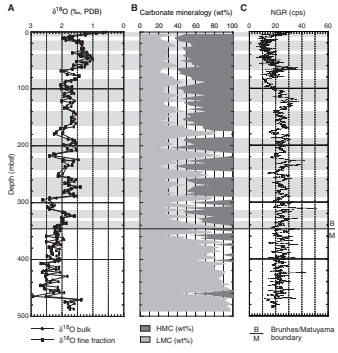

RESULTS AND DISCUSSION

Stable Isotope Results

The $\delta^{18}O$ values for bulk and fine fractions (<38 µm) are presented vs. depth (Figs. F1, F3). The upper 340 m of the record is characterized by distinct cyclicity, whereas the record below 340 mbsf is marked by high-frequency, low-amplitude variations. Bulk- and fine-fraction $\delta^{18}O$ data closely follow each other, with the bulk samples generally showing slightly more negative values. Bulk- and fine-fraction $\delta^{18}O$ values show an overall range from 2.9‰ to 0.4‰. An upward trend toward more negative values is visible in both $\delta^{18}O$ records.

The $\delta^{13}C$ isotope values from bulk and fine fractions (<38 µm) are presented vs. depth (Fig. F2). The upper 150 mbsf of the $\delta^{13}C$ record is marked by high-frequency, high-amplitude fluctuations, which are followed by a 150-m interval with little variation. Below 300 mbsf, $\delta^{13}C$ values shift –1‰, and the remaining curve is again characterized by high-frequency, high-amplitude variations. As previously observed for $\delta^{18}O$ values, bulk- and fine-fraction $\delta^{13}C$ values follow each other, with the bulk having a slightly more negative value. Overall, $\delta^{13}C$ values range from 2.0‰ to 0.25‰. The carbon isotope record is presented but is not discussed further in this data report.

Downhole Comparison

The transition between the Holocene and the last glacial maximum (LGM) is evident in the $\delta^{18}O$ record, with an amplitude change of 1.4‰, comparable to global data sets. Except for Termination I, amplitudes, especially in the upper part of the record (20–170 mbsf), are small (<±0.5‰) and variable, but they increase again between 170 and 320 mbsf. In summary, the bulk- and fine-fraction isotopes do not record glacial–interglacial changes on a magnitude of other global, mostly pelagic, records. The reason could lie within the continental-shelf environment and the composition of the bulk- and fine-fraction samples from Site 1127. Although containing abundant planktonic and benthic foraminifers as well as calcareous nannoplankton, the sediment is dominated by the bioclastic fragments of the benthic-shelf community.

A comparison with the lithostratigraphy of Site 1127 (Feary, Hine, Malone, et al., 2000) provides a possible explanation as to why Termination I is better expressed compared with the underlying record. Lithostratigraphic Unit I (0–9.6 mbsf) consists of calcareous ooze with varying amounts of nannofossils and planktonic foraminifers, whereas Unit II (9.6–467.2 mbsf) is marked by alternating wackestone and packstone sediments. The change in Unit II is, therefore, characterized by an increase in grain size and bioclast abundance and a decrease in carbonate mud. The presented data illustrate the need for a stable isotope analysis based on planktonic and benthic foraminifers in order to validate the bulk- and fine-fraction data and discuss the record in a stratigraphic and paleoceanographic context.

Initial shipboard comparison of mineralogic and seismic downhole logging data indicates cyclic packaging of the Pleistocene sediment wedge, probably in response to orbitally driven sea level fluctuations (Feary, Hine, Malone, et al., 2000). By comparing isotopic data with other sea level–proxy data sets, this hypothesis can be tested. In Figure

F3, we made a first-order correlation of the three data sets, as indicated by gray and white bars. Based on shipboard bulk analysis, the carbonate mineralogy shows large variations within the high-Mg calcite (HMC) and low-Mg calcite (LMC) percentages (Feary, Hine, Malone, et al., 2000). Variations are most obvious in the relative percentages of HMC and LMC that are characterized by an interfingering behavior and are especially pronounced in the interval between 165 and 320 mbsf. Here, HMC-dominated intervals correspond to times of decreased isotopic values (sea level highstands) and LMC-dominated intervals to times of increased isotopic values (sea level lowstands). Although the mineralogical variations also fluctuate in the upper part of the record (0–65 mbsf), no consistent trend or interfingering behavior is observed. Note that the LGM and Termination I are both HMC dominated. Fluctuations within the NGR record in comparison with the isotope stratigraphy and mineralogical data are less pronounced; nevertheless, most abrupt decreases or increases in NGR counts can be correlated to mineralogic and isotopic changes. Below the B/M boundary, the decreased amplitude of the isotopic fluctuations and the abrupt increase of LMC are interpreted as the result of diagenetic alteration and remineralization.

From a comparison of the $\delta^{18}O$ results, carbonate mineralogy, and NGR records, we conclude that (1) for the middle part of the record (between the B/M boundary at 343.4 and 165 mbsf), the cyclic behavior of LMC, HMC, and NGR fluctuations vary systematically with fluctuations observed in the oxygen isotope record; (2) the upper part of the record (165–10 mbsf), where amplitudes within the isotopic record are small and variable, correlates to an HMC-dominated time as seen in the mineralogic record; (3) the LGM is well defined in all three data sets; and (4) below the B/M boundary, diagenetic overprinting has eliminated the original signal.

Comparison to SPECMAP

In order to test the potential usefulness of cool-water shelf carbonates for paleoceanographic studies, we have correlated the Hole 1127B $\delta^{18}O$ record to the orbitally tuned SPECMAP $\delta^{18}O$ curve (Imbrie et al., 1984) (Fig. F4). Depths and ages of isotope boundaries that were used as tie points are listed in Table T2. The correlation for the LGM is convincing, but it is poorer for marine isotope Stages (MISs) 3–11, where glacial–interglacial amplitudes are small. The mid-Pleistocene (MISs 12–17) correlation improves as glacial–interglacial amplitudes rise, and within MIS 15, even internal structures are visible. The reason for the poor correlation is most likely related to the strong neriticly influenced signal in the Site 1127 bulk and fine fractions opposed to the predominantly pelagic planktonic foraminiferal values of the SPECMAP curve. We, nevertheless, tentatively identify 20 MISs down to the level of the shipboard observed B/M boundary (Feary, Hine, Malone, et al., 2000).

Although this data set is preliminary, it represents a first attempt at developing a bulk- and fine-fraction isotope stratigraphy for the cool-water carbonate realm of the GAB. It illustrates the need for more precise stable isotope analysis of specific planktonic and benthic foraminifers in order to evaluate the true potential of these sediments as sensitive recorders of global ice volume fluctuations. Based on the promising results of this initial study, a stable isotope analysis of foraminifers is currently in progress to interpret paleoclimate fluctuations on the GAB.

F4. Comparison of the late Pleistocene $\delta^{18}O$ stratigraphies from SPECMAP and Hole 1127B, p. 10.

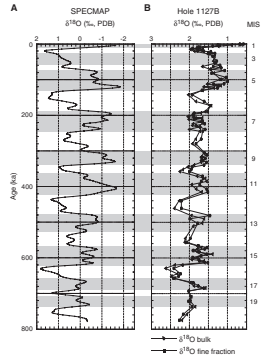

T2. Estimated depth of the marine isotope stages (MIS), Hole 1127B, p. 13.

ACKNOWLEDGMENTS

This research used samples and/or data provided by the Ocean Drilling Program (ODP). ODP is sponsored by the U.S. National Science Foundation (NSF) and participating countries under management of Joint Oceanographic Institutions (JOI), Inc. Funding for this research was provided by ETH Research Project No. 0-20-506-98.

We thank the crew and Shipboard Scientific Party of ODP Leg 182 for their tremendous effort in the recovery of Site 1127 sediments. We thank D.A. Feary and one anonymous reviewer for their thoughtful comments, which improved the manuscript.

REFERENCES

Feary, D.A., Hine, A.C., Malone, M.J., et al., 2000. *Proc. ODP, Init. Repts.,* 182 [CD-ROM]. Available from: Ocean Drilling Program, Texas A&M University, College Station, TX 77845-9547, U.S.A.

Imbrie, J., Hays, J.D., Martinson, D.G., McIntyre, A., Mix, A.C., Morley, J.J., Pisias, N.G., Prell, W.L., and Shackleton, N.J., 1984. The orbital theory of Pleistocene climate: support from a revised chronology of the marine $\delta^{18}O$ record. *In* Berger, A., Imbrie, J., Hays, J., Kukla, G., and Saltzman, B. (Eds.), *Milankovitch and Climate* (Pt. 1), NATO ASI Ser. C, Math Phys. Sci., 126:269–305.

Shackleton, N.J., Hall, M.A., Pate, D., Meynadier, L., and Valet, J.-P., 1993. High resolution stable isotope stratigraphy from bulk sediment. *Paleoceanography,* 8:141–148.

Figure F1. Bulk- and fine-fraction (<38 µm) $\delta^{18}O$ record from Hole 1127B. PDB = Peedee Belemnite.

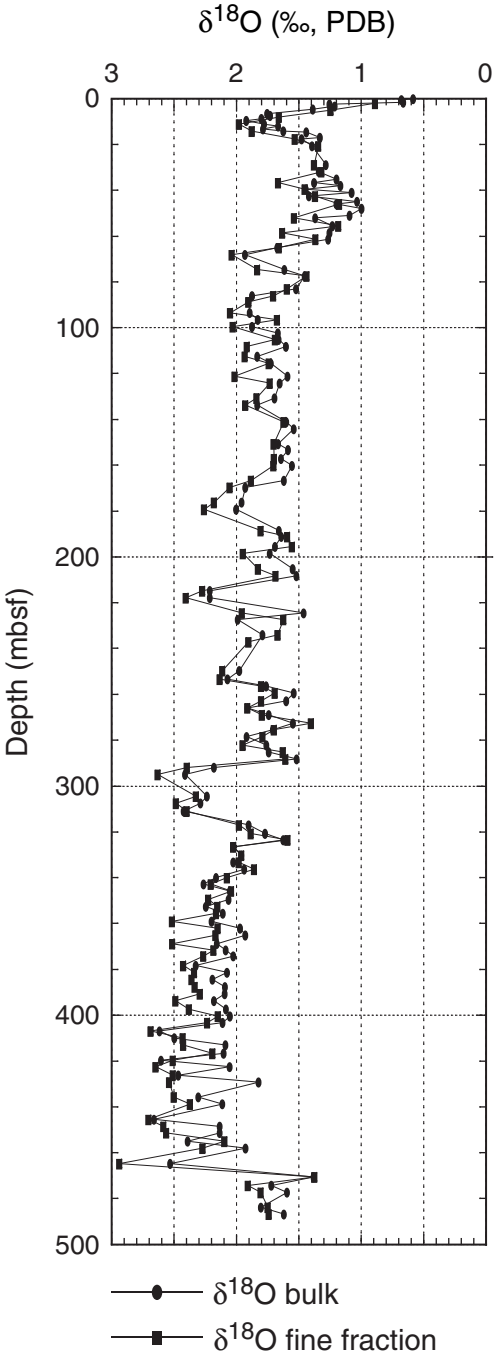

Figure F2. Bulk- and fine-fraction (<38 µm) $\delta^{13}C$ record from Hole 1127B. PDB = Peedee Belemnite.

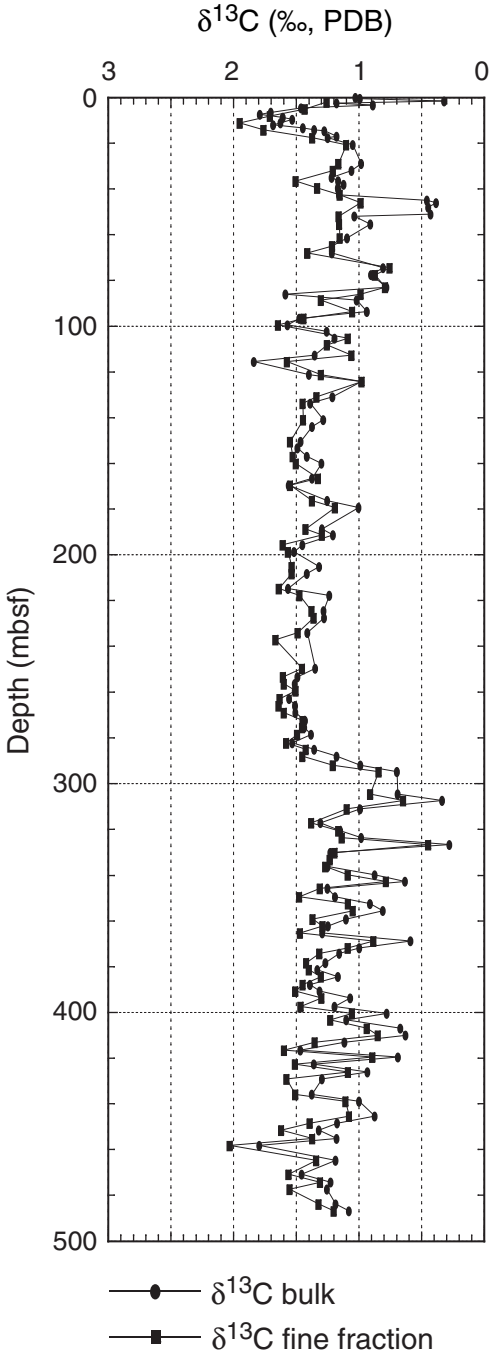

Figure F3. Comparison of Hole 1127B data: (**A**) $\delta^{18}O$ stratigraphy, (**B**) mineralogical, and (**C**) downhole logging natural gamma ray (NGR) shipboard data. PDB = Peedee Belemnite, cps = counts per second, HMC = high-Mg calcite, LMC = low-Mg calcite.

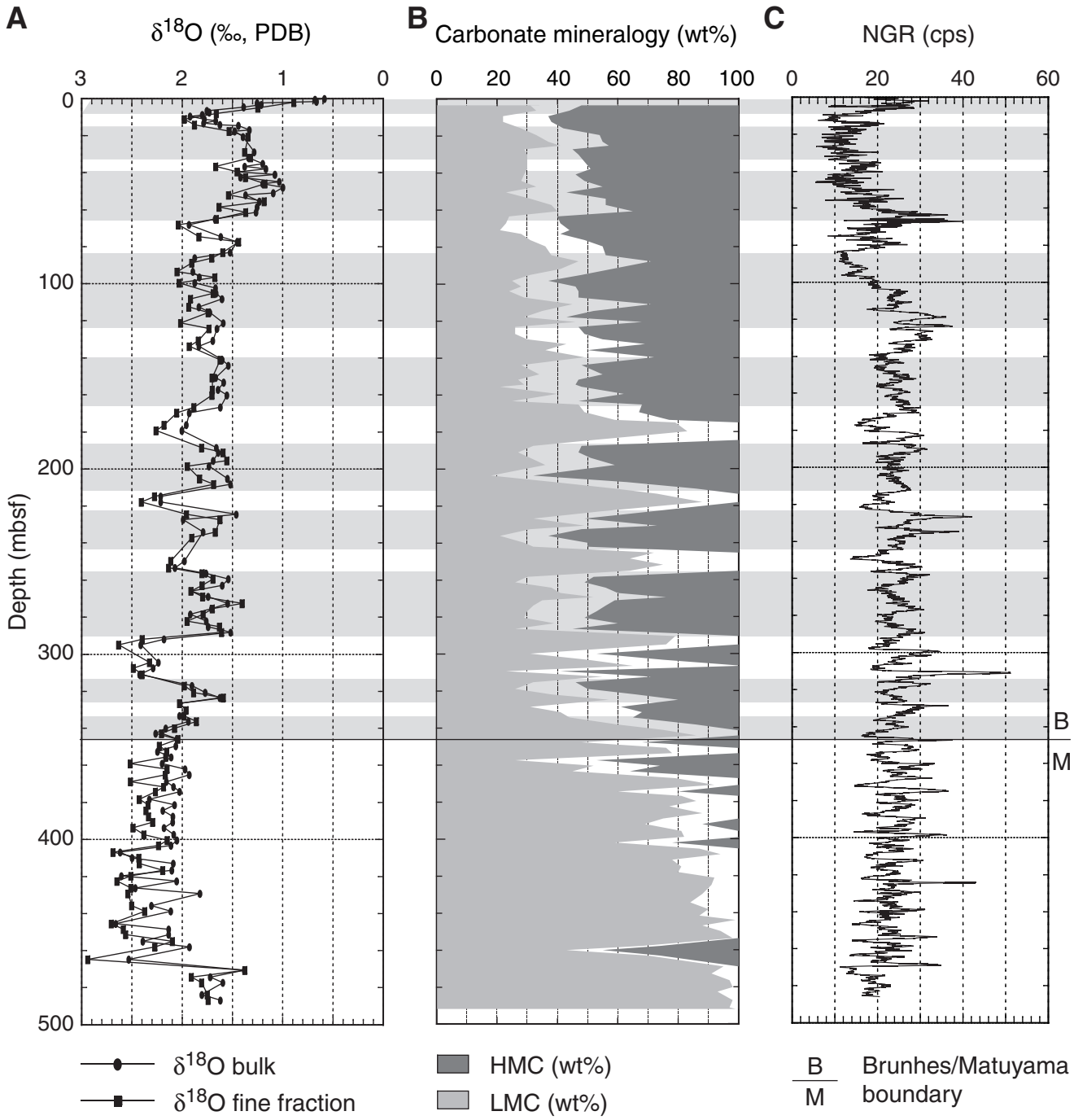

Figure F4. Comparison of the late Pleistocene $\delta^{18}O$ stratigraphies from (**A**) SPECMAP (Imbrie et al., 1984) and (**B**) Hole 1127B. The marine isotope stages (MIS) are indicated. PDB = Peedee Belemnite.

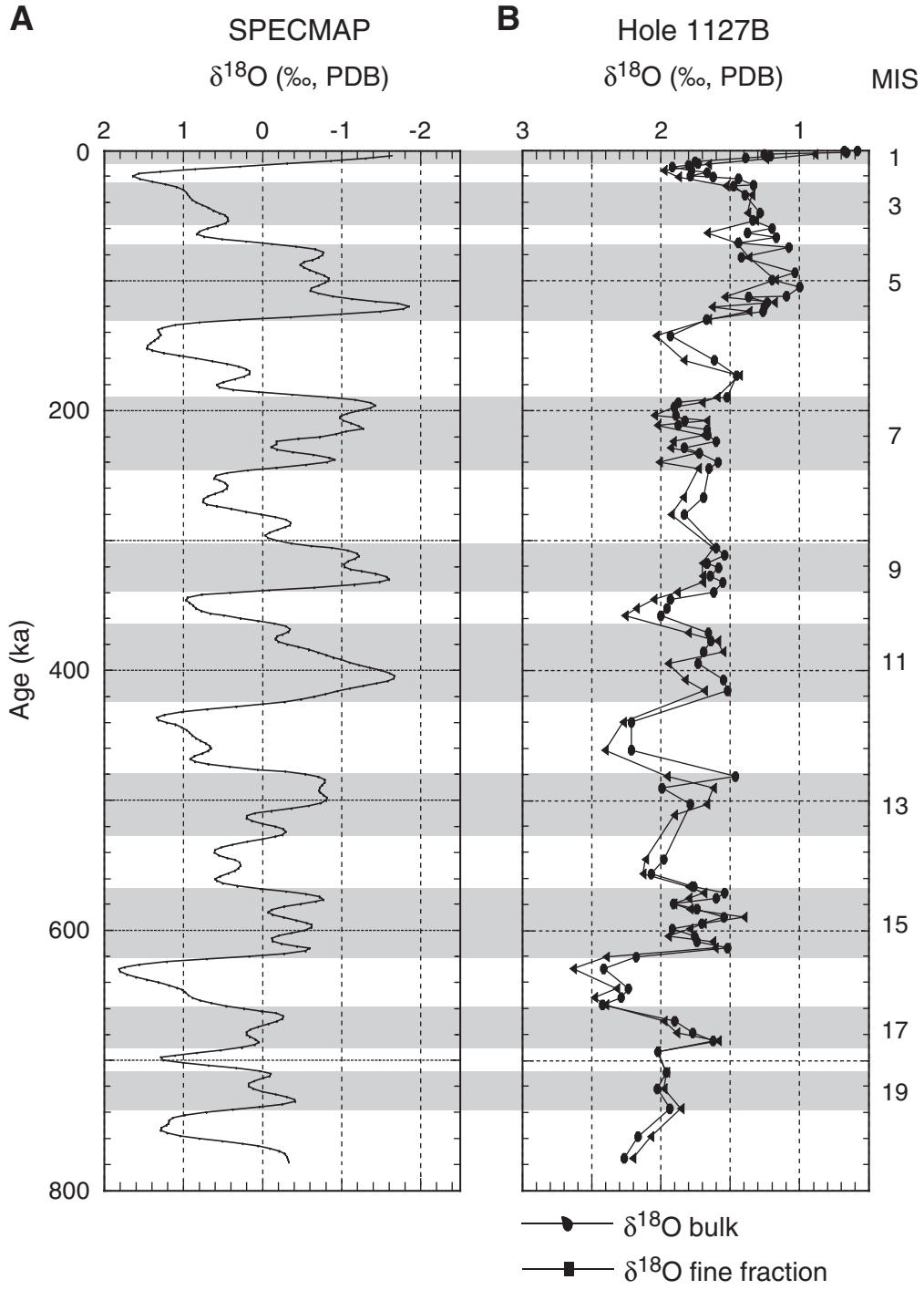

Table T1. Results of stable isotope analyses, Hole 1127B. (**See table note.** Continued on next page.)

Core, section, interval (cm)	Depth (mbsf)	$\delta^{13}C$ bulk (‰ PDB)	$\delta^{18}O$ bulk (‰ PDB)	$\delta^{13}C$ ff (‰ PDB)	$\delta^{18}O$ ff (‰ PDB)
182-1127B-					
1H-1, 2–6	0.02	1.03	0.58		
1H-1, 50–53	0.50	0.99	0.68		
1H-2, 2–	1.52	0.32	0.66		
1H-2, 101–106	2.51	1.18	1.25		
1H-3, 46–49	3.46	0.89	1.21		
1H-4, 2–7	4.52	1.46	1.39		
2H-1, 69–75	6.59	1.70	1.75		
2H-2, 2–7	7.42	1.79	1.73		
2H-2, 139–144	8.79	1.61	1.80		
2H-3, 70–75	9.60	1.53	1.92		
2H-4, 65–70	11.05	1.63	1.78	1.95	1.98
2H-5, 2–5	11.92	1.68	1.67		
2H-6, 2–8	13.42	1.45	1.79		
2H-6, 65–70	14.05	1.36	1.62	1.76	1.88
2H-6, 125–130	14.65	1.28	1.44		
3H-2, 3–8	16.93	1.18	1.33		
3H-2, 65–70	17.55	1.25	1.48	1.37	1.53
3H-4, 65–70	20.55	1.05	1.39	1.10	1.35
4H-4, 65–70	28.98	0.98	1.28	1.16	1.38
4H-6, 64–69	31.97	1.06	1.34	1.21	1.32
5H-1, 75–80	35.15	1.22	1.20		
5H-2, 65–70	36.55	1.16	1.38	1.50	1.67
5H-3, 60–65	38.00	1.12	1.17		
5H-4, 62–67	39.52	1.17	1.44	1.33	1.45
5H-5, 60–65	41.00	1.16	1.08		
5H-6, 65–70	42.55	1.16	1.42	1.15	1.37
6H-1, 110–115	45.00	0.46	1.03		
6H-2, 65–70	46.05	0.38	1.20	0.99	1.18
6H-3, 110–115	48.00	0.45	1.00		
6H-5, 110–115	51.00	0.43	1.09		
6H-6, 65–70	52.05	1.04	1.37	1.16	1.54
7H-2, 65–70	55.55	0.91	1.23	1.16	1.18
7H-4, 65–70	58.55	0.49	1.25	0.29	1.63
7H-6, 59–64	61.49	1.10	1.26	1.15	1.37
8H-2, 65–70	65.05	1.21	1.67	1.21	1.66
8H-4, 64–69	68.04	1.21	1.93	1.41	2.04
9H-2, 65–70	74.55	0.81	1.62	0.76	1.83
9H-4, 65–70	77.55	0.90	1.45	0.87	1.44
10H-2, 65–70	82.94	0.78	1.52	0.79	1.60
10H-4, 65–70	85.94	1.59	1.88	0.99	1.71
10H-6, 38–43	88.67	1.02	1.90	1.30	1.90
11H-2, 65–70	93.55	0.94	1.89	1.05	2.05
11H-4, 65–70	96.55	1.48	1.83	1.44	1.67
11H-6, 70–75	99.44	1.57	1.87	1.64	2.03
12H-2, 65–70	102.29	1.26	1.67		
12H-4, 64–69	105.28	1.19	1.66	1.09	1.69
12H-6, 66–71	108.20	1.25	1.60	1.26	1.92
13H-2, 66–71	112.56	1.35	1.83	1.06	1.93
13H-4, 66–71	115.49	1.84	1.73	1.57	1.74
14H-2, 65–70	121.20	1.40	1.59	1.30	2.02
14H-4, 65–70	124.20	0.98	1.65	0.98	1.73
15H-2, 65–70	130.81	1.21	1.69	1.34	1.84
15H-4, 65–70	133.81	1.39	1.83	1.45	1.93
16H-2, 65–70	141.05	1.28	1.60	1.45	1.62
16H-4, 65–70	144.05	1.37	1.54		
17X-2, 65–70	150.55	1.47	1.67	1.55	1.70
17X-4, 61–66	153.34	1.49	1.59		
18X-2, 65–70	157.05	1.42	1.64	1.53	1.70
18X-4, 65–70	160.05	1.30	1.55	1.50	1.70
19X-2, 65–70	166.65	1.37	1.62	1.33	1.88
19X-4, 65–70	169.65	1.56	1.93	1.55	2.05
20X-2, 65–70	176.25	1.25	1.96	1.37	2.18
20X-4, 68–73	179.28	1.00	2.00	1.19	2.26
21X-4, 66–71	188.57	1.29	1.66	1.43	1.81
21X-6, 68–73	191.17	1.21	1.64	1.29	1.59
22X-2, 65–70	195.55	1.45	1.69	1.61	1.55
22X-4, 65–70	198.55	1.52	1.73	1.56	1.95
23X-2, 65–70	205.15	1.32	1.55	1.54	1.83
23X-4, 65–70	208.15	1.42	1.52	1.54	1.69
24X-2, 65–70	214.75	1.56	2.21	1.64	2.27
24X-4, 65–70	217.75	1.24	2.21	1.47	2.40
25X-2, 65–70	224.45	1.28	1.46	1.38	1.96
25X-4, 65–70	227.45	1.28	1.99	1.36	1.62
26X-2, 65–70	234.05	1.41	1.79	1.49	1.67
26X-4, 65–70	237.05	1.20	1.08	1.67	1.90
27X-2, 65–70	243.65				
27X-4, 63–67	246.63	0.67	0.21		
27X-6, 64–69	249.64	1.35	1.98	1.45	2.11
28X-2, 65–70	253.25	1.49	2.07	1.61	2.13
28X-4, 65–70	256.25	1.51	1.76	1.60	1.80
28X-6, 66–70	259.26	1.51	1.54	1.51	1.69
29X-2, 65–70	262.95	1.56	1.60	1.63	1.80
29X-4, 65–70	265.95	1.51	1.91	1.64	1.91
29X-6, 65–70	268.95	1.51	1.74	1.60	1.79
30X-2, 65–70	272.55	1.43	1.55	1.45	1.40
30X-4, 64–69	275.54	1.44	1.71	1.45	1.70
30X-6, 65–70	278.55	1.38	1.92	1.49	1.79
31X-2, 65–70	282.15	1.53	1.76	1.58	1.95
31X-4, 64–69	285.14	1.36	1.74	1.42	1.63
31X-6, 65–70	288.15	1.18	1.52	1.45	1.61
32X-2, 66–68	291.86	0.99	2.18	1.21	2.40
32X-4, 64–66	294.84	0.70	2.41	0.84	2.63
33X-2, 63–68	301.43				
33X-4, 62–67	304.42	0.69	2.24	0.91	2.32
33X-6, 62–67	307.42	0.33	2.29	0.65	2.48
34X-2, 65–70	311.05	0.99	2.42	1.10	2.40
34X-4, 65–70	314.05				
34X-6, 66–71	317.06	1.31	1.90	1.38	1.98
35X-2, 65–70	320.65	1.15	1.77	1.16	1.89
35X-4, 65–70	323.65	0.98	1.62	1.14	1.59
35X-6, 66–71	326.66	0.28	2.02	0.45	2.03
36X-2, 67–69	330.27	1.23	1.96	1.19	1.96
36X-4, 65–70	333.25	1.23	2.02	1.23	1.98
36X-6, 65–70	336.25	1.25	1.94	1.27	1.86
37X-2, 65–70	339.85	0.87	2.16	1.09	2.08
37X-4, 65–70	342.85	0.63	2.26	0.78	2.21
37X-6, 66–71	345.86	1.25	2.05	1.31	2.04
38X-2, 66–71	349.46	1.19	2.06	1.48	2.23
38X-4, 66–71	352.46	0.91	2.24	1.09	2.15
38X-6, 67–72	355.47	0.81	2.11	1.05	2.16
39X-2, 65–70	359.15	1.10	2.20	1.37	2.52
39X-4, 65–70	362.15	1.25	1.97	1.29	2.15
39X-6, 67–69	365.17	1.29	1.93	1.47	2.17
40X-2, 65–70	368.75	0.59	2.16	0.88	2.51
40X-4, 65–70	371.75	1.00	2.09	1.09	2.18
40X-6, 61–64	374.21	1.16	2.03	1.32	2.27
41X-2, 65–70	378.35	1.27	2.33	1.42	2.43
41X-4, 65–70	381.35	1.33	2.07	1.40	2.34
41X-6, 65–70	384.35	1.17	2.19	1.30	2.36
42X-2, 65–70	387.75	1.39	2.09	1.45	2.33
42X-4, 65–70	390.75	1.31	2.09	1.51	2.29
42X-6, 67–72	393.77	1.07	2.18	1.30	2.49
43X-2, 65–70	397.35	1.19	2.08	1.46	2.38
43X-4, 65–70	400.35	0.78	2.05	1.06	2.15
43X-6, 65–69	403.35	1.10	2.11	1.23	2.24
44X-2, 65–71	406.95	0.67	2.62	0.94	2.69
44X-4, 64–69	409.94	0.63	2.50	0.85	2.43
44X-6, 66–71	412.96	1.12	2.09	1.35	2.43
45X-2, 66–71	416.56	1.47	2.10	1.60	2.19
45X-4, 66–71	419.56	0.69	2.60	0.89	2.51
45X-6, 66–71	422.56	1.36	2.05	1.51	2.65
46X-2, 64–68	426.14	0.93	2.47	1.09	2.51
46X-4, 65–69	429.15	1.29	1.82	1.58	2.54
47X-2, 65–70	435.85	1.38	2.31	1.51	2.50
47X-4, 65–70	438.85	1.00	2.11	1.11	2.37
48X-2, 65–70	445.45	0.87	2.66	1.08	2.70
48X-4, 65–70	448.45	1.17	2.13	1.39	2.58

Table T1 (continued).

Core, section, interval (cm)	Depth (mbsf)	$\delta^{13}C$ bulk (‰ PDB)	$\delta^{18}O$ bulk (‰ PDB)	$\delta^{13}C$ ff (‰ PDB)	$\delta^{18}O$ ff (‰ PDB)
48X-6, 66–71	451.46	1.32	2.13	1.62	2.56
49X-2, 65–70	455.05	1.18	2.39	1.37	2.10
49X-4, 65–70	458.05	1.79	1.93	2.03	2.27
50X-2, 65–68	464.65	1.19	2.53	1.34	2.94
50X-6, 66–69	470.66	1.46	1.38	1.56	1.38
51X-2, 65–70	474.25	1.23	1.72	1.31	1.91
51X-4, 65–70	477.25	1.25	1.59	1.55	1.81
52X-2, 65–70	483.85	1.19	1.80	1.32	1.75
52X-4, 64–69	486.84	1.08	1.62	1.20	1.74

Note: ff = fine fraction, PDB = Peedee Belemnite.

Table T2. Estimated depth of the marine isotope stages (MISs), Hole 1127B.

MIS	Age (ka)	Depth (mbsf)
2	12	9.2
3	24	16
4	59	34.5
5	71	40.5
6	128	65.5
7	186	83
8	245	125
9	303	140
10	339	167
11	362	185
12	423	212
13	478	223
14	524	243
15	565	256
16	620	292
17	659	312
18	689	325
19	710	334
20	736	347

Note: Ages are in thousands of years (ka) and based on Imbrie et al. (1984).